journal

J. Am. Ceram. Soc., 78 [10] 2763–68 (1995)

Metalorganic Chemical Vapor Deposition by Pulsed Liquid Injection Using an Ultrasonic Nozzle: Titanium Dioxide on Sapphire from Titanium(IV) Isopropoxide

Vera A. Versteeg,[*,†,‡] C. Thomas Avedisian,[§] and Rishi Raj[*,†]

Department of Materials Science and Engineering, and Department of Mechanical and Aerospace Engineering, Cornell University, Ithaca, New York 14853

A new method for metalorganic chemical vapor deposition has been developed in which a precursor solution is directly injected into a reaction chamber. The vaporization of short pulses of liquid is facilitated by atomization with a piezoelectrically operated nozzle. The system has been used successfully to grow oriented, thin TiO_2 (rutile) films on sapphire substrates with the crystalline relationship $(101)[010]_R \parallel (11\bar{2}0)[0001]_S$. A film growth rate of approximately 2.5 monolayers of TiO_2 (rutile) per pulse was achieved at 650°C for a reactant impingement rate of about 250 monolayers of $Ti(OPr^i)_4$ per pulse.

I. Introduction

Metalorganic chemical vapor deposition (MOCVD) techniques have come into increasing use in recent years, due to the growing versatility and availability of precursors and improved environmental advantages over the halogenated compounds used for conventional CVD. Most commonly, the films are deposited by dissolving the metalorganic reactant (typically a metal alkoxide) in a carrier gas, which is carried through heated lines to a heated substrate.[1] The metal alkoxides decompose by pyrolysis, leaving the metal oxide. While this method has been used to produce excellent epitaxial films, it has the disadvantages of complexity: the precursor must be heated to fix its vapor pressure, the gas flow rate carefully controlled, and the carrier lines heated to prevent condensation before reaching the reactor. Additionally, this conventional method cannot be used with certain low-volatility precursors that decompose upon heating.

Various techniques have been used to overcome some of these difficulties. Titanium dioxide films have been grown by a direct liquid injection method, in which the precursor, in dilute solution, is introduced into a heated antechamber, where it evaporates and diffuses to the heated substrate below.[2] However, this process is difficult to control, in terms of both injection and evaporation rates.

Other examples of liquid or solution precursor CVD are based on spray pyrolysis techniques, and not limited to metalorganic precursors. In some cases, an ultrasonic nebulizer is substituted for the gas bubbler: the carrier gas brings a fine mist to the reaction chamber where it evaporates.[3,4] In other cases, a spray solution is injected directly into the reaction chamber, generally at atmospheric pressure.[5,6]

In this work, we present a new MOCVD process that improves upon the above techniques, adding features of direct, pulsed on/off liquid injection in conjunction with atomization by an ultrasonic, piezoelectrically driven nozzle, in a low-pressure environment. The pulsed injection allows control of film deposition rates, as fine as monolayers per pulse. The waiting time between pulses can be designed to allow time for atomic rearrangements by diffusion on the growth surface. The ultrasonic nozzle adds the capability for reproducibly vaporizing the liquid in the reactor. The low pressure facilitates the uniformity of deposition on large substrates, and enhances the evaporation of the solution precursor.

To demonstrate the feasibility of this process, and to develop and characterize the performance of the reactor, titanium(IV) isopropoxide ($Ti(OPr^i)_4$) was chosen as a precursor of TiO_2 to deposit on sapphire substrates. This system is well documented in the literature, and both the high- and low-temperature phases of TiO_2 (rutile and anatase, respectively) grow epitaxially on sapphire, depending on temperature and substrate orientation.[7] TiO_2 has the useful properties of a high refractive index and a high dielectric constant; on sapphire it can be used for oxygen sensors.[8] It can be grown by oxidizing[6] or hydrolyzing[9] $TiCl_4$. Its most common metalorganic precursor is $Ti(OPr^i)_4$, due largely to its high vapor pressure (bp 49°C at 0.1 torr).[10]

In this paper, we present the results of TiO_2 films grown using this pulsed, liquid injection method. The operation of the reactor is described, and the reactant impingement rates are compared to actual deposition rates. Finally, the resulting films are shown to be comparable in quality to those grown by conventional MOCVD, at similar growth rates and a fraction of the expense.

II. Reactor Design

For this work, we constructed a prototype, low-pressure reactor. The system consists of four "modules": (i) the pulsed ultrasonic liquid injector, (ii) the cold-wall reactor and vacuum system, (iii) the substrate heater, and (iv) a computer interface and console for process control. The key features of this system are illustrated schematically in Fig. 1.

The unique feature of this reactor is the liquid injection system, which allows the precursor to be pulsed directly into the reactor in small quantities, then atomized reproducibly by the nozzle. The precursor is prepared in the form of a dilute solution; a mixture of 0.03 to 0.30 mol% $Ti(OPr^i)_4$ in toluene is typical. The solution was prepared according to a method similar to that reported in Ref. 2. This solution, and a pure solvent for line purging, are kept in isolated reservoirs (not shown in Fig. 1), which can be selected electrically by a solenoid valve. Inert gas (Ar) from a regulated, low-pressure line is used as a displacement medium to push the liquid through the container outlet and then the pulsing mechanism.

A. I. Kingon—contributing editor

Manuscript No. 194162. Received October 4, 1993; approved June 28, 1994.
Supported by the National Science Foundation under Grant No. DDM-9400180 and by the New York State Science and Technology Foundation (RDG 92110) with additional funds from Sono-Tek Corp., Poughkeepsie, NY. This work made use of MRL Central Facilities supported by the National Science Foundation under Award No. DMR-9121654.

*Member, American Ceramic Society.
†Department of Materials Science and Engineering.
‡Now at CVC Products, Inc., Rochester, New York.
§Department of Mechanical and Aerospace Engineering.

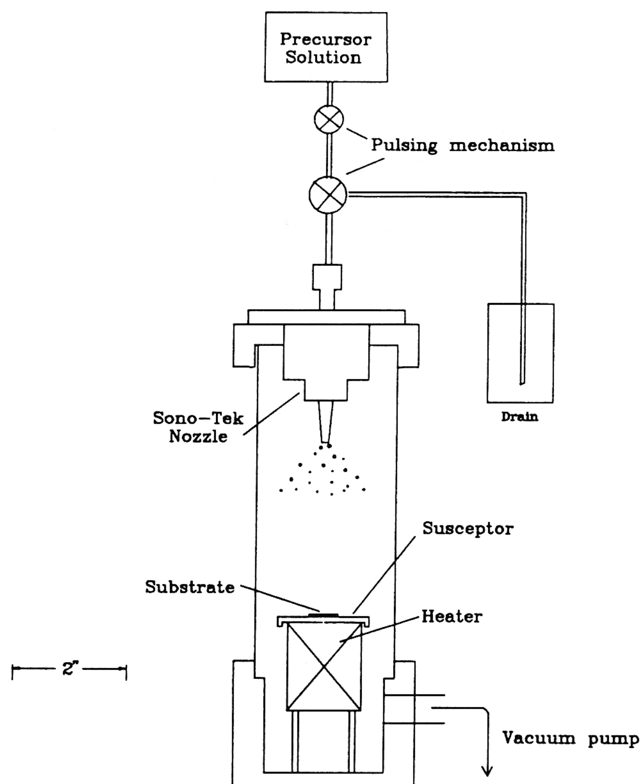

Fig. 1. Schematic diagram of the MOCVD system. The scale bar is shown to indicate its compactness.

The pulsing mechanism consists of two computer-controlled solenoid valves, operating in tandem. When the first (two-way) valve is open, the liquid runs through a short storage line, with the excess draining out the normally open port of the second (three-way) valve. Then, the first valve is closed, and subsequently the second valve is activated, releasing the contents of the storage line to the chamber. The pressure differential between the line and the chamber (at vacuum) forces the liquid through the nozzle, where the solution is atomized. The timing of the valves can be tuned for efficient use of precursor and optimal film growth. The volume injected is reproducible for a given valve timing, and measures about 5 μL per pulse. The amount of waste generated is very small, and is disposed of through appropriate means.

The reproducibility and control over the injection rate is significantly enhanced by the ultrasonic nozzle (manufactured by Sono-Tek Corp., Poughkeepsie, NY). It is a single-fluid nozzle: mechanical vibrations, rather than pressure, provide energy for atomization. The nozzle contains piezoelectric transducers that create standing vibrations along the straight bore of the nozzle body. These vibrations set up standing waves in the liquid, with amplitude that increases along the nozzle body and reaches a maximum at the nozzle tip. There the liquid is thrown off, into the reaction chamber, in a fine mist of droplets of approximately 20 μm mean diameter.[11] Once in the chamber, the droplets evaporate rapidly; thus only vapor comes into contact with the substrate. A calculation of the average evaporation time and travel distance of a droplet is included in the Appendix.

The reactor itself consists of a cold-wall quartz tube. It is maintained at a base pressure of 0.01 torr and an operating pressure of 0.1–1 torr under continuous pumping by a rotary pump. The reduced pressures allow uniform film growth and enhanced vaporization of the precursor solution. Condensibles, including solvent vapor and reaction byproducts, are removed from the exhaust with a cold trap. Pressure is measured with a capacitance manometer.

The existing heater is capable of 700°C susceptor temperature. It consists of an infrared lamp surrounded by layers of metal heat shielding. The susceptor is made of stainless steel; atop it is clamped the substrate, which is heated by conduction.

A computer console is interfaced to the CVD reactor, with software to control the temperature of the substrate, the pulse rate, and the shape of the duty cycle for film gowth. The pressure and temperaure of the chamber are continuously recorded during deposition.

III. Pulsed Liquid Injection

The nozzle makes it possible to apply the concept of pulsed liquid injection. This concept is to inject a measured amount of reactant into the chamber, which rapidly vaporizes, causing the pressure to increase, as illustrated schematically in Fig. 2. The vapor is removed by continuous pumping, and the chamber pressure returns to its baseline value. After a waiting time t_w, another liquid pulse is injected, and the process repeats.

Ideally, the amount of precursor injected is designed to result in one equivalent monolayer of deposition per pulse. From kinetic gas theory, the cumulative impingement of molecules, n_i, of a given species i per unit area depends on the integrated species partial pressure p_i with respect to time t.

$$n_i = \frac{1}{\sqrt{2\pi m_i kT}} \int p_i(t)\, dt \qquad (1)$$

where T is temperature, k is Boltzmann's constant, and m_i is the molecular mass.

An analytical relation for the precursor impingement rate, in monolayers of reactant per pulse, can be derived assuming that the pressure p has an infinitely fast rise time at $t = 0$, and then an exponential decay at $t > 0$, offset by the chamber base pressure p_0:

$$p = p_0 + \Delta p = p_0 + \Delta p_{max} e^{(-t/\tau)} \qquad (2)$$

where Δp is the change in chamber pressure due to the evaporating liquid and τ is the time constant for decay, related to the pumping speed.

Since only the pulsed pressure contributes to the reactant flux, p_0 can be neglected. The pressure change can be integrated over the course of one pulse, from $t = 0$ to $t = t_w$, to give the cumulative impingement

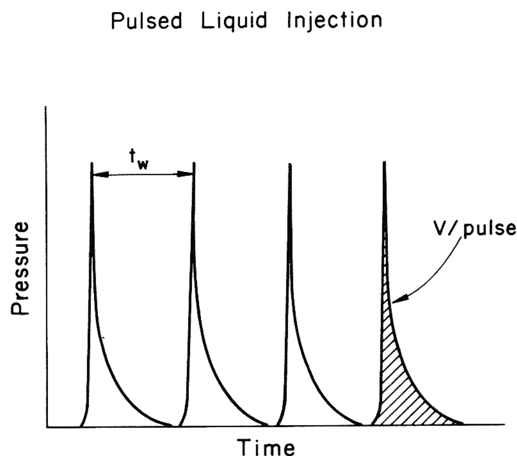

Fig. 2. Ideal pressure response of a reaction chamber to periodic, pulsed liquid injection. When the injection begins, atomization-enhanced evaporation is nearly instantaneous, and pressure rises sharply. After the liquid supply is cut, the pressure falls exponentially to its base level. Another pulse begins after waiting time t_w. The area under each pulse can be related to the total number of molecules injected per pulse, by the use of Eq. (1).

$$\int_0^{t_w} \Delta p \, dt = \Delta p_{max} \tau (1 - e^{-t_w/\tau}) \quad (3)$$

It is assumed that the partial pressure of the metalorganic reactant in the chamber is proportional to its concentration in solution, i.e., $p_{mo} = c_{mo} p$. The impingement in monolayers, of precursor molecules, is proportional to the adsorbed molecular area A_{mo}. This area can be estimated from molecular volume V_{mo}, which depends on the precursor liquid density, ρ_{mo}. The shape of the volume can be approximated as a cube, in which case $A_{mo} = V_{mo}^{2/3}$. Thus, the impingement per pulse in monolayers (N_{mo}) is given by

$$N_{mo} = \frac{m_{mo}^{1/6} c_{mo}}{\rho_{mo}^{2/3} \sqrt{2\pi k T}} [\Delta p_{max} \tau (1 - e^{-t_w/\tau})] \quad (4)$$

The waiting time between pulses can be optimized to obtain ordered growth, allowing sufficient time for atomic rearrangements on the substrate. Practically, t_w must be larger than τ to achieve the pulsed effect and to avoid overloading the vacuum system. However, it should be sufficiently short to obtain useful film deposition rates.

The experimentally observed pressure response of the chamber is shown in Fig. 3, which demonstrates the vaporization effect of the ultrasonic nozzle. The dashed lines indicate the response with the nozzle operating normally—their functional form matches the expected response depicted in Fig. 2, and is regular and reproducible from peak to peak. In contrast, if the nozzle power is off, no atomization occurs, and the nozzle bore acts merely as a feed tube. In this case, the pressure fluctuates widely from pulse to pulse. Under these conditions, large droplets were observed to coalesce and fall from the nozzle after every few pulses.

IV. Results: The Growth of TiO_2

Films of titanium dioxide were grown under the following general conditions: susceptor temperature 700°C (substrate temperature approximately 650°C); chamber pressure 0.1–1 torr, as shown in Fig. 3; t_w = 5 or 20 s; precursor concentration 0.03 mol% $Ti(OPr^i)_4$ in toluene; for 135 to 1000 pulses.

(1) Growth Rate

The pressure was recorded as a function of time during all of the depositions; numerical integration of these data according to Eqs. (1) to (3) indicate that the impingement rate of $Ti(OPr^i)_4$ was 255 ML per pulse average with 120 ML/pulse standard deviation. This rate was calculated from Eqs. (1) to (4) assuming the evaporation temperature T = 300 K, $m_{mo} = 4.72 \times 10^{-22}$ kg, ρ^{mo} = 0.952 g/cm^3, p_0 = 0.01 torr, and $c_{mo} = 3 \times 10^{-4}$.

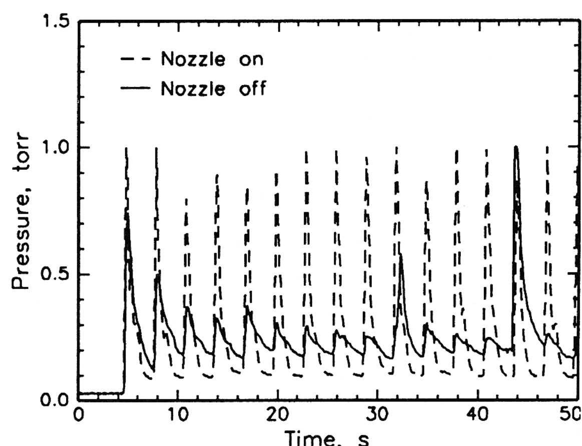

Fig. 3. Influence of the ultrasonic nozzle on the reproducibility of pulsed injection and vaporization.

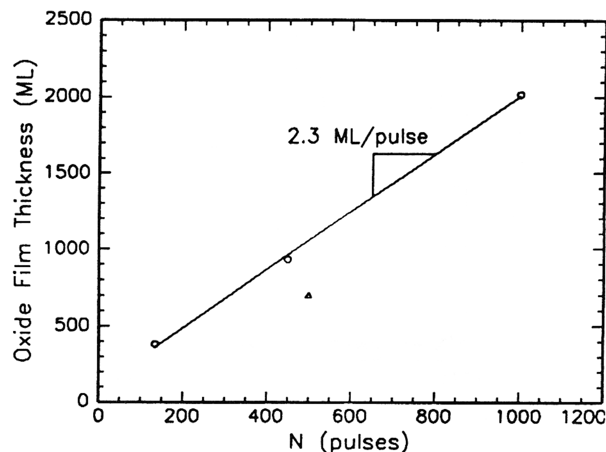

Fig. 4. Film thickness as a function of number of deposition pulse cycles: (○) t_w = 5 s, (△) t_w = 20 s.

The integrated pressure with respect to time was calculated numerically, directly from the recorded data, and was found to range from 90 to 200 Pa·s per pulse.

The thicknesses of the resulting films were measured by Rutherford backscattering spectroscopy (RBS). This analysis technique measures the number of atoms deposited per unit area; the thickness can be calculated by assuming the film is fully dense rutile (an assumption confirmed by the following X-ray and TEM results). These thicknesses are plotted as a function of number of pulses in Fig. 4. These data show a linear relationship with number of doses for t_w = 5 s; the per-pulse growth rate is somewhat lower for t_w = 20 s. In the former case, the average deposition rate is 2.5 ± 0.6 ML/pulse, less than 1/100 of the precursor impingement rate.

(2) Structure of the Overgrowth

All of the depositions produced transparent films with several thickness fringes. X-ray normal scans, as shown in Fig. 5, revealed that the films were highly oriented, with (101) rutile parallel to the (11$\bar{2}$0) sapphire. In some cases, a $\{200\}_R$ reflection was also detected, at much lower intensities.

To measure the mosaic spread, rocking curves, or θ-scans, were performed on the $\{101\}_R$ reflection of the film. For a film grown for 450 pulses with t_w = 5 s, the observed FWHM (full width, half-maximum peak) value was 0.1°, as illustrated in Fig. 6(a). This result is compared with one grown by conventional MOCVD, Fig. 6(b), from the same precursor on the same

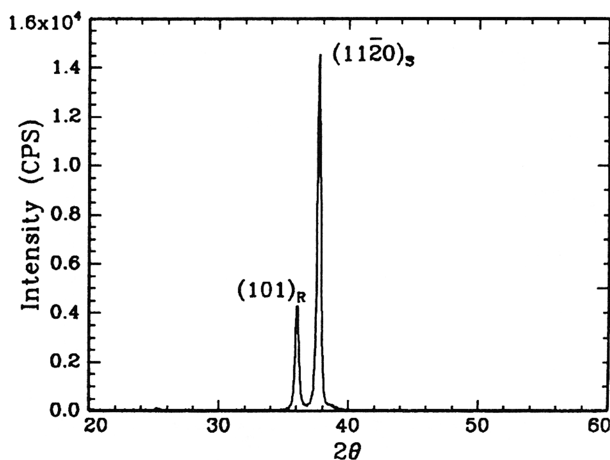

Fig. 5. X-ray normal scan results. Radiation used was Cu$K\alpha_1$, with wavelength 1.54 Å. The rutile 101 peak is at 36.1°, and the sapphire 11$\bar{2}$0 peak is at 37.8°.

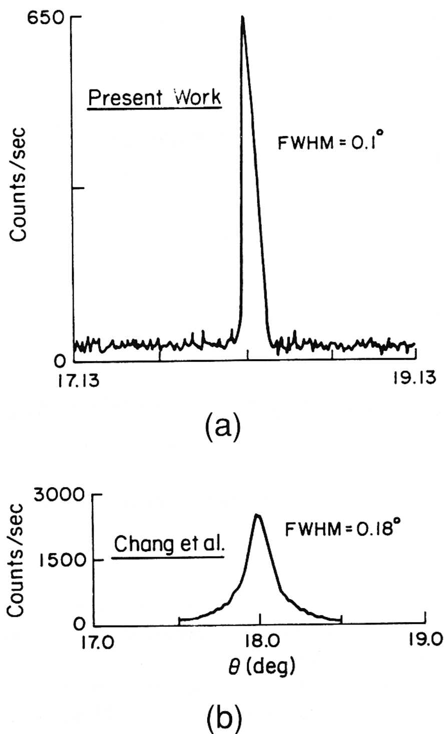

Fig. 6. (a) Rocking curve on the above 101_R film peak (450 pulses, 5-s pulse interval). (b) Rocking curve from a comparable film grown by conventional MOCVD (Ref. 1).

substrate (FWHM = 0.18°).[1] Thus, the two have a similar degree of orientation.

The orientation of the films, within the plane of the interface, was determined from X-ray pole figure analysis. The pole figures from the $\{11\bar{2}6\}_S$ planes of the substrate and the $\{121\}_R$ planes of the above-mentioned film have been converted to ϕ-scans, which are shown in Fig. 7. The $(11\bar{2}6)_S$ and $(11\bar{2}0)_S$ planes share a zone axis of $[1\bar{1}00]_S$. The $(121)_R$ and $(101)_R$ share the $[10\bar{1}]_R$ zone axis. The poles from both film and substrate have the same ϕ-rotation, indicating that these zone axes are parallel. It follows from the crystallography, illustrated in Fig. 8, that the normal directions to the zone axes within the plane of the interface are parallel, too, i.e., $[010]_R \parallel [0001]_S$.

This result is confirmed by cross-sectional transmission electron microscopy (TEM) in Fig. 9. This figure was taken from a film grown for 500 pulses and t_w = 20 s, but otherwise similar conditions to the film whose results are presented above. This film consisted of oriented crystallites of approximately 25 nm in diameter and a 180 nm film thickness. The interface is abrupt and shows an excellent lattice match in the plane of the figure: $3[10\bar{1}]_R$ = 1.638 nm and $2[1\bar{1}00]_S$ = 1.648 nm, yielding a −0.6% mismatch. The lattice match in the orthogonal direction is also favorable: $3[010]_R$ = 1.377 nm and $1[0001]_S$ = 1.299 nm, yielding a +6.0% mismatch.

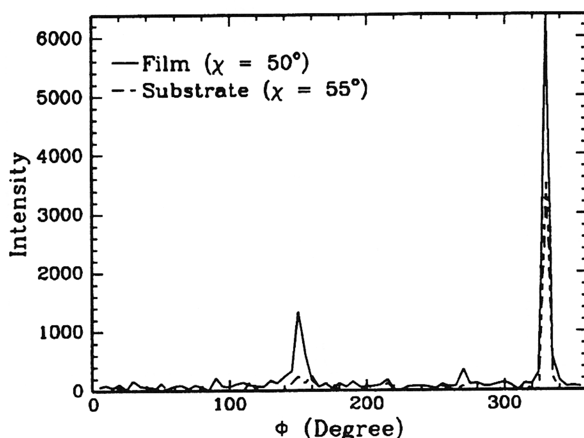

Fig. 7. X-ray ϕ-scans of $11\bar{2}6$ sapphire and (121) rutile, from the above film.

In MOCVD, one important issue is the presence of residual carbon from the precursor in the oxide film. While the above characterization techniques do not directly detect carbon, it may be inferred from the high quality of the results that it is present only in insignificant quantities. Auger analysis of TiO_2 films grown from $Ti(OPr^i)_4$ under UHV conditions shows a decrease in incorporated carbon with increasing deposition temperature, and at temperatures of 500°C and greater, carbon levels lie at or below the detection limit.[12]

V. Discussion

(1) Growth Rate

The discrepancy between impingement and deposition rates may be explained partially by the volume change between a precursor and oxide molecule: the equivalent volume of TiO_2 is about 1/6 the volume of a $Ti(OPr^i)_4$ molecule. The rest of the difference, which amounts to a factor of about 40, reflects the low reaction probability for adsorption and pyrolysis of the $Ti(OPr^i)_4$ molecules on the surface of the substrate. The rate of production of TiO_2 molecules, $\dot{N}_{ox}$, expressed in units of monolayers per unit time, may be written in terms of N_{mo}, the number of monolayers of the metalorganic molecules on the surface, in the following form:

$$\dot{N}_{ox} = N^n_{mo} v_1 e^{(-Q_{pyr}/RT)} \tag{5}$$

where n is the order of the reaction, v_1 is the vibration frequency parallel to the substrate plane, and Q_{pyr} is the activation energy barrier for the pyrolysis reaction.

The surface metalorganic concentration N_{mo} may be written in terms of the impingement rate of the alkoxide molecules on the substrate, Γ_{mo}, as

$$N_{mo} = \frac{\Gamma_{mo}}{v_2} e^{(Q_{ad}/RT)} \tag{6}$$

where v_2 is the vibration frequency normal to the substrate plane, and Q_{ad} is the adsorption energy of the alkoxide molecules to the surface. Note that the quantity N_{mo} in Eq. (4) is the time integral of Γ over the duration of the pulse. Taken together, Eqs. (5) and (6) suggest that a low value for Q_{ad} and/or a high Q_{pyr} for pyrolysis can reduce the rate of oxide deposition. Systematic experiments are now under way in our laboratory to measure the activation parameters and n for this class of MOCVD reactions.

(2) Process Control

The process variables in the pulsed, liquid injection MOCVD reactor are N_{mo}, the impingement rate of the metal alkoxide molecules in units of monolayers per pulse; t_w, the waiting time from pulse to pulse; and T_s, the substrate temperature.

The quantity N_{mo} is given by Eq. (4). It depends on τ, determined by the pump-down characteristics of the system; ΔV, the amount of reactant solution injected per pulse; and c_{mo}, the concentration of the precursor in the reactant solution. An important advantage of the present MOCVD design is that N_{mo}, and therefore the deposition rate, can be changed by several orders of magnitude. For example, in the current experiment the following parameters were used: $\Delta V = 5$ μL and $c_{mo} = 3 \times 10^{-4}$; the pumping system consisted of a simple mechanical roughing pump. These conditions led to $N_{mo} \approx 255$ monolayers per pulse. A factor of 10^3 increase in deposition rate could be obtained simply by using the pure precursor. The volume unit ΔV could also be easily increased by a factor of 10^1–10^2. On the other hand, N_{ML} could be reduced by using a pump with a higher throughput and by reducing ΔV by a factor of 10. Taking

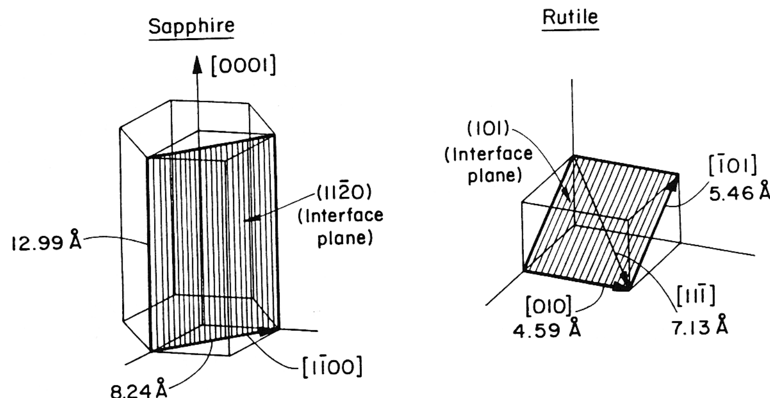

Fig. 8. Schematic unit cells of sapphire and rutile. The interface planes are shaded; major directions and their lattice parameters are indicated. In these films, $(101)[010]_R \parallel (11\bar{2}0)[0001]_S$.

these together, it is likely that the system can yield deposition rates that span a factor of 10^7, making it useful not only for epitaxial growth but also for the growth of thick films.

The optimization of the waiting time t_w and the substrate temperature T_s will depend on the atomistic mechanisms of nucleation and growth. An oxide molecule produced by pyrolysis on the surface must migrate, by surface diffusion, to the nearest growth site on the growing crystal(s). If these sites on the surface have an average spacing λ, then the requirement for epitaxial growth is that the characteristic oxide surface diffusion length be greater than λ:

$$4D_{s,o}e^{(-Q_s/RT_s)}t_w > \lambda^2 \quad (7)$$

where $D_{s,o}$ is the surface diffusion coefficient of the oxide and Q_s its activation energy. The pulsing feature of the reactor offers greater control for improving epitaxy: t_w can be made sufficiently long to allow enough time for a few oxide molecules to find epitaxial sites on the overgrowth, before new ones are introduced in the next pulse.

VI. Summary

The new technique of pulsed, liquid injection, even in its earliest stages of development, has proved to be an extremely simple, economical means of growing highly oriented oxide films. It builds on the strength of MOCVD, the availability of safe oxide precursors, while avoiding its disadvantages: the need for cumbersome mass flow controllers, carrier gases, heated sources and lines, and a high-throughput pumping system. A compact, table-top reactor can produce uniform, oriented films, with monolayer-by-monolayer control, with no loss in quality compared to conventional MOCVD. This performance is made possible by using the ultrasonic atomizing nozzle to enhance the vaporization of the precursor solution.

This paper presents the results of the growth of rutile on sapphire, a well-characterized system. The deposition system is versatile, and can be used for any type of film. Its capability for epitaxy makes it ideal for ferroelectric films; oriented $LiTaO_3$ has already been grown on sapphire.[13] In addition, the reactor is expandable to a multinozzle configuration for multiple sources to produce layered and doped structures.

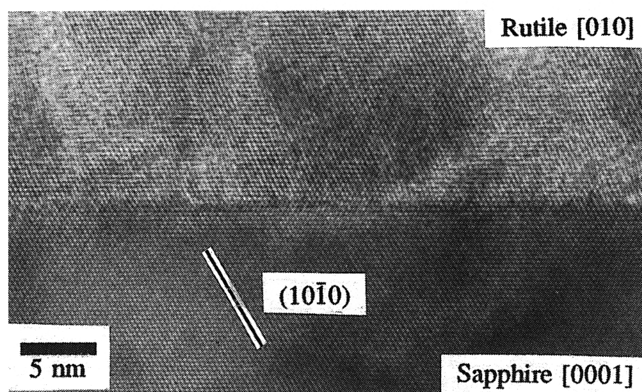

Fig. 9. Cross-sectional TEM micrograph of a similar rutile film (500 pulses, 20-s pulse interval). The interface is abrupt, and the film and substrate show an excellent lattice match.

APPENDIX

Droplet Lifetime

The lifetime of a droplet under vacuum can be estimated by the following method: it is assumed that a droplet is injected into an atmosphere of negligible pressure relative to the equilibrium partial pressure exerted by the droplet. This pressure is given by

$$p_{eq} = p_0 e^{\frac{2\gamma\Omega}{rkT}} \quad (8)$$

where p_0 is the partial pressure of a flat surface of the liquid in question, γ is the surface tension of the liquid (assumed to be curvature independent), Ω is the molecular volume, and r is the droplet radius. The exponential term accounts for the extra pressure exerted by the curvature of the droplet.

From kinetic gas theory, the molecular flux through a unit area can be estimated in the direction normal to the droplet surface:

$$\Gamma_{ev} = \frac{p_{eq}}{(2\pi mkT)^{1/2}} \quad (9)$$

where Γ_{ev} is the evaporative flux in particles/area/time, and m is the mass of the particle. Since it is assumed that the pressure at some distance from the droplet is negligible, the total flux away from the droplet can be equated with its change in volume due to evaporation:

$$\frac{dV}{dt} = -\Gamma_{ev}A\Omega \quad (10)$$

where V is the droplet volume and A is its area.

Substituting in the droplet radius r and rearranging,

$$\frac{dt}{dr} = \frac{(2\pi mkT)^{1/2}}{\Omega p_0} e^{\frac{-2\gamma\Omega}{rkT}} \quad (11)$$

The time for a droplet to evaporate from its initial radius r_0 to some final radius r_f can be calculated by integrating

$$t_{ev} = \int_{0}^{t_{ev}} dt = B \int_{r_0}^{r_f} e^{-A/r}\, dr \tag{12}$$

where

$$A = \frac{2\gamma\Omega}{kT} \tag{13a}$$

$$B = \frac{(2\pi mkT)^{1/2}}{\Omega p_0} \tag{13b}$$

The integration is accomplished through a series solution

$$t_{ev} = B \int \left[1 - \frac{A}{r} + \frac{A^2}{2!r^2} - \frac{A^3}{3!r^3} + \ldots + (-1)^n \frac{A^n}{n!r^n} \right] dr \tag{14}$$

yielding the result

$$t_{ev} = B \left[r - A \ln r - \frac{A^2}{2!r} + \frac{A^3}{2 \cdot 3!r^2} - \ldots + (-1)^{n-1} \frac{A^n}{(n-1)n!r^{n-1}} \right]_{r_0}^{r_f} \tag{15}$$

The lifetime of a 10 μm radius droplet of pure toluene is calculated, using values of

$$m = \frac{MW}{N_A} = 1.53 \times 10^{-25}\ \text{kg}$$

$$T = 300\ \text{K}$$

$$\rho_l = 0.87 \frac{\text{g}}{\text{cm}^3}$$

$$\Omega = \frac{m}{\rho_l} = 1.76 \times 10^{-28}\ \text{cm}^3$$

$$r_f = \sqrt[3]{\frac{3\Omega}{4\pi}} = 3.5 \times 10^{-10}\ \text{m}$$

$$p_0 = 5300\ \text{Pa}$$

$$\gamma = 2.74 \times 10^{-2} \frac{\text{N}}{\text{m}}$$

$$r_0 = 10\ \mu\text{m} \tag{16}$$

giving an estimated time of evaporation $t_{ev} = 6.8 \times 10^{-4}$ s (the values for p_0 and γ are given in Ref. 14).

To calculate the distance of travel from the nozzle into the chamber, it is necessary to estimate the average velocity of the droplets as they leave the nozzle. The following conditions are assumed; the average droplet velocity is the same as the average velocity $\bar{v}$ of the stream of liquid as it travels down the nozzle bore of diameter $d = 3.8 \times 10^{-4}$ m and length $L = 5$ cm; the atomization does not change this velocity; drag forces on the droplets in the chamber are minimal; and the entire pressure drop ΔP of the liquid, from atmospheric to vacuum, occurs along this nozzle bore.

From elementary fluid mechanics, the head loss in a circular pipe with turbulent flow is given by[15]

$$h_f = \frac{\Delta P}{\rho_l} = f \frac{L}{d} \frac{\bar{v}^2}{2g} \tag{17}$$

where f is a friction factor, depending on the pipe diameter and roughness, and g is the gravitational constant. Solving for $\bar{v}$, using $f = 0.04$ (for drawn tubing, and Reynolds number $Re \approx 10^4$), and assuming $\Delta P = 1.01 \times 10^5$ Pa, and pure toluene liquid, yields a velocity of 21 m/s. Combined with $t_{ev} = 6.8 \times 10^{-4}$ s above, the droplet travel distance is 1.4 cm, approximately the distance the spray was observed visually. This value represents an approximate upper limit, since additional drag forces due to the liquid delivery system are not taken into account. In any case, this distance is much smaller than the length of the reactor (approximately 25 cm from the nozzle to the substrate), verifying that only vapor, not droplets, comes into contact with the substrate.

Acknowledgments: The high-resolution transmission electron micrograph in Fig. 9 was obtained by Huyang Xie. Assistance from Glenn Swan in the building of the reactor is gratefully acknowledged.

References

[1]H. L. M. Chang, H. You, Y. Gao, J. Guo, C. M. Foster, R. P. Chiarello, T. J. Zhang, and D. J. Lam, "Structural Properties of Epitaxial TiO_2 Films Grown on Sapphire $(11\bar{2}0)$ by MOCVD," *J. Mater. Res.*, **7** [9] 2495–506 (1992).

[2]J.-P. Lu, J. Wang, and R. Raj, "Solution Precursor Chemical Vapor Deposition of Titanium Oxide Thin Films," *Thin Solid Films*, **204**, L13–15 (1991).

[3]E.g., C. H. Lee and S. J. Park, "Preparation of Ferroelectric $BaTiO_3$ Thin Films by Metal Organic Chemical Vapour Deposition," *J. Mater. Sci.: Mater. Electron.*, **1**, 219–24 (1990).

[4]L. D. McMillan, C. A. Paz de Araujo, T. Roberts, J. Cuchiaro, M. C. Scott, and J. F. Scott, "Liquid Source CVD," *Integr. Ferroelectr.*, **2**, 351–59 (1992).

[5]W. J. DeSisto and R. L. Henry, "Preparation and Characterization of MgO Thin Films Deposited by Spray Pyrolysis of Mg(2,4-pentanedionate)$_2$," *J. Cryst. Growth*, **109**, 314–17 (1990).

[6]S. Zhang, Y. F. Zhu, and D. E. Brodie, "Photoconducting TiO_2 Prepared by Spray Pyrolysis Using $TiCl_4$," *Thin Solid Films*, **213**, 265–70 (1992).

[7]H. L. M. Chang, H. You, J. Guo, and D. J. Lam, "Epitaxial TiO_2 and VO_2 Films Prepared by MOCVD," *Appl. Surf. Sci.*, **48/49**, 12–18 (1991).

[8]E. M. Logothetis and W. J. Kaiser, "TiO_2 Film Oxygen Sensors Made by Chemical Vapour Deposition from Organometallics," *Sens. Actuators*, **4**, 333–40 (1983).

[9]K. S. Yeung and Y. W. Lam, "A Simple Chemical Vapour Deposition Method for Depositing Thin TiO_2 Films," *Thin Solid Films*, **109**, 169–78 (1983).

[10]D. C. Bradley, R. C. Mehrotra, and P. D. Gaur, *Metal Alkoxides*; p. 63. Academic Press, London, U.K., 1978.

[11]Sono-Tek product literature.

[12]J.-P. Lu and R. Raj, "Ultra-High Vacuum Chemical Vapor Deposition and *In Situ* Characterization of Titanium Oxide Films," *J. Mater. Res.*, **6** [9] 1913 (1991).

[13]H. Xie and R. Raj, "Epitaxial $LiTaO_3$ Thin Film by Pulsed MOCVD from a Single Precursor," *Appl. Phys. Lett.*, **63**, 3146–48 (1993).

[14]N. B. Vargaftik, "Handbook of Physical Properties of Liquids and Gases," 2nd ed.; pp. 347–48. Hemisphere Publishing Corp., New York, 1975.

[15]F. M. White, *Fluid Mechanics*, 2nd ed.; pp. 302–16. McGraw-Hill, New York, 1986. □